Physica B 189 (1993) 99–110
North-Holland

SDI: 0921-4526(93)E0013-B

PHYSICA B

Charging effects in quantum dots at high magnetic fields

N.C. van der Vaart, A.T. Johnson[1], L.P. Kouwenhoven[2], D.J. Maas, W. de Jong, M.P. de Ruyter van Steveninck, A. van der Enden and C.J.P.M. Harmans
Department of Applied Physics, Delft University of Technology, Delft, The Netherlands

C.T. Foxon[3]
Philips Research Laboratories, Redhill, Surrey, UK

We have studied charging effects in quantum dots, defined by gates in the two-dimensional electron gas of an AlGaAs–GaAs heterostructure. We have investigated Coulomb oscillations at zero magnetic field, and in the integer and fractional QHE regimes. Coulomb oscillations are found to appear only when both barrier conductances G are below the first well resolved plateau: at zero field $G < 2e^2/h$, in the IQHE regime $G < e^2/h$, and in the FQHE regime $G < \frac{1}{3}e^2/h$. The period of the oscillations is shown to be field independent. We furthermore studied the interplay between charging effects and discrete energy states in the dot. In the IQHE, we found a regular pattern in the amplitude of the Coulomb oscillations that corresponds to the number of Landau levels in the dot. In a smaller dot containing only 25 electrons, the excitation spectrum of the dot is investigated at finite source–drain voltages.

1. Introduction

Transport through a small isolated island reveals several interesting effects. The discrete nature of the electron charge leads to the Coulomb blockade [1] and size quantization yields discrete energy states in the island [2,3], leading to effects as coherent resonant tunneling. The classical charging effects in metallic structures, where size quantization can be ignored, are presently well understood [4]. A semiconductor quantum dot is a particularly interesting system, because deviations from the classical model can arise. Moreover, different magnetic field regimes can be studied from zero field up to the integer and fractional quantum Hall effect (QHE) regimes.

At low temperatures, transport through the dot can be strongly regulated by charging effects. Adding one electron to the dot costs a finite charging energy which makes it possible to control the number of electrons in the dot and to change them one by one. Coulomb effects can in this way serve as a new tool to investigate transport phenomena. For instance, McEuen et al. [5,6] used this method to map out the magnetic field dependence of the Nth electron ground state in the integer QHE regime. It also opens new ways of studying many body effects, such as the fractional QHE [7].

In this paper we present experiments on quantum dots defined by split-gates in a two-dimensional electron gas (2DEG). In section 2, we describe our quantum dot geometry, and in section 3 we provide a brief review of the theory for charging effects. Section 4 contains experimental results in the linear transport regime. In section 4.1, we examine the conditions necessary to observe charging effects. We will focus on

Correspondence to: N.C. van der Vaart, Department of Applied Physics, Delft University of Technology, P.O. Box 5046, 2600 GA Delft, The Netherlands.
[1] Present address: Dir. 814.03 NIST, 325 Broadway, Boulder, CO 80303, USA.
[2] Present address: Lawrence Berkeley Laboratories, Mailstop 2-200, Berkeley, CA 94720, USA.
[3] Present address: Department of Physics, University of Nottingham, Nottingham NG7 2RD, UK.

the role of quantized conductance and magnetic field. In section 4.2, we investigate the period of the Coulomb oscillations as a function of the magnetic field. Furthermore, we study the structure in the amplitude of the Coulomb oscillations in the IQHE regime. The presence of discrete energy states, sometimes referred to as zero-dimensional (0D) states, in the dot is reflected in a regular pattern in the amplitude modulation. In section 5 we present non-linear transport measurements which show direct evidence for the existence of 0D states in a quantum dot containing approximately 25 electrons. In section 6 we discuss and summarize our results.

2. Split-gate quantum dot

Fig. 1 shows a SEM photograph of the split-gate geometry fabricated on top of a GaAs/AlGaAs heterostructure with a 2DEG 100 nm below the surface. The ungated 2DEG has a mobility of $2.3 \times 10^6\,\mathrm{cm^2/V\,s}$ and an electron density of $1.9 \times 10^{15}\,\mathrm{m^{-2}}$ at 4.2 K. We denote gate F as the finger gate, gates 1 to 3 as quantum point contact (QPC) gates, and gate C_1 and C_2 as the center gates. In the experiments we describe in this paper, QPC3 and the center gate C_2 are not used: they are grounded and have no effect on the 2DEG. Applying −400 mV to gates F, C_1, 1, and 2 depletes the electron gas underneath them and forms a quantum dot with a diameter of about 800 nm. The narrow channels between gates 1–C_1, and 2–C_1 are pinched-off at this gate voltage. Electron transport occurs only through the QPC constrictions induced by gates 1–F, and 2–F, which couple the dot to the two wide 2DEG regions. This structure allows us to characterize the QPC conductances individually by only applying a voltage to the finger gate F and to one of the QPC gates. Making the gate voltages more negative reduces the dot size to a diameter of roughly 600 nm.

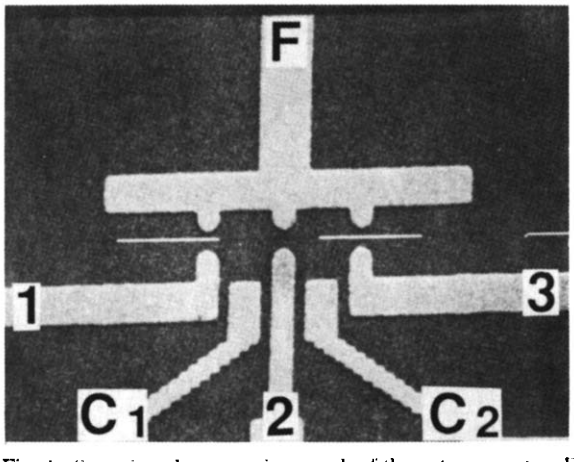

Fig. 1. Scanning electron micrograph of the gate geometry: F denotes the finger gate, 1 to 3 the QPC gates, and C_1 and C_2 the center gates. QPC gate 3 and C_2 are not used. The white marker has a length of 1 μm.

The largest energy associated with the addition of one electron to the dot is the charging energy e^2/C, which is a classical estimate for Coulomb interactions. An estimate of the total capacitance C of the dot to ground can be obtained from the self-capacitance of a disc $C_0 = 4\varepsilon_0\varepsilon_r d$. For a dot with a diameter $d = 600$ nm and $\varepsilon_r = 13$ in GaAs, $C_0 = 2.8 \times 10^{-16}$ F and the charging energy $e^2/C_0 = 0.6$ meV. At temperatures below 4 K, the charging energy is the dominant energy scale.

From the ungated 2DEG electron density and the area of the dot, we estimate that the number of electrons in the dot is approximately 500. This implies that the second relevant energy, which is the average separation between the 0D states in the dot, is about $E_F/500 = 0.01$ meV, where the Fermi energy E_F is 7 meV. Although the charging energy far exceeds the energy splitting of the 0D states, we will demonstrate that both energies have specific and distinguishable effects on the transport properties of the dot.

3. Theory of charging effects

We briefly review the theory dealing with charging effects in quantum dots. More detailed discussions of the theory can be found in recent literature [1,8–10] where the charging theory for metal systems is generalized to take into account the discrete spectrum of the energy states in a quantum dot.

Fig. 2 illustrates the potential landscape of the dot induced by the gates. The states in the

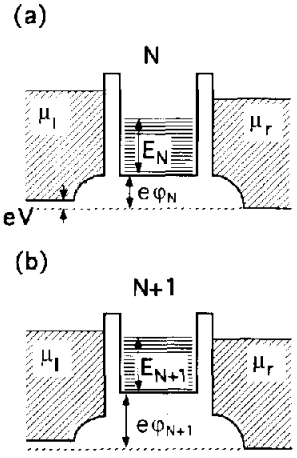

Fig. 2. Potential landscapes in the 2DEG induced by the gates. μ_l and μ_r are the potentials of the leads. φ_N is the electrostatic potential with N electrons in the dot. $V = (\mu_l - \mu_r)/e$ is the source–drain voltage across the sample. Adding one electron to the dot in (a) increases the electrostatic potential $e\varphi_N$ by e^2/C and results in (b). The extra electron occupies the 0D state E_{N+1}.

reservoirs are filled up to the electrochemical potentials μ_l and μ_r. The energy separation between the 0D states is $E_{N+1} - E_N$. For sufficiently small barrier conductances, the electrons in the dot are strongly localized and the number of electrons in the dot can only change by an integer. When an extra electron tunnels into the dot, the electrochemical potential $\mu_d(N)$ of the dot changes by $\mu_d(N+1) - \mu_d(N) = E_{N+1} - E_N + e^2/C$ [10]. At zero temperature, transport through the dot can be blocked by this energy gap. It is only possible to add the $(N+1)$th electron to the dot (fig. 2(a)) when the final position of the $(N+1)$th 0D state lines up with μ_l and μ_r (fig. 2(b)). Transport takes place via the states with N (fig. 2(a)) and $N+1$ (fig. 2(b)) electrons in the dot. Note that the extra electron occupies the $(N+1)$th 0D state and that the conduction band increases with e^2/C: $e\varphi_{N+1} - e\varphi_N = e^2/C$.

By changing the electrostatic potential φ_N in the dot with the gate voltage, the final position of the $(N+1)$th 0D state will no longer line up with μ_l and μ_r. Transport is now blocked. As the gate voltage is swept, the conductance of the dot oscillates between zero (blockade) and non-zero (no blockade). These oscillations are known as Coulomb oscillations. Each period corresponds to a change of one electron in the dot.

If the thermal energy $k_b T$ is less than the level spacing $E_{N+1} - E_N$, tunneling occurs primarily through one particular 0D state. If this process takes place coherently, the resonant dot conductance can far exceed the individual barrier conductances. In the charging regimes, the dot conductance can approach the maximum value of e^2/h, when both barriers are equal. That this maximum is e^2/h instead of $2e^2/h$ is not due to a spin effect, but results from the correlation between subsequent tunnel events: first an electron must tunnel out before the next electron can tunnel into the dot.

4. Experiments in the linear transport regime

4.1. Conditions on the barrier conductance for the occurrence of Coulomb oscillations

The conductance of a QPC at zero magnetic field is quantized in units of $2e^2/h$, due to the formation of 1D subbands [11]. Fig. 3(a) shows the conductances G_1 of QPC_1 and G_2 of QPC_2 as a function of the gate voltage on QPC 1 and 2, respectively. The voltages on the finger gate F and the center gate C_1 are kept constant, and there is zero voltage applied to the other gates [12]. The measurements are performed in zero magnetic field at a temperature of 10 mK, using an ac lock-in technique. Both G_1 and G_2 show a quantized plateau at $2e^2/h$. Only below the plateau, electrons in the lowest 1D subband have a non-zero probability to be reflected by the QPC.

In fig. 3(b), the conductance of the dot is measured as a function of the center gate voltage with fixed voltages on QPC1 and 2, and the finger gate F. The conductance of QPC_2 is for all curves set to about e^2/h and the conductance of QPC_1 is successively set to the values denoted by the arrows in fig. 3(a). In curve (a) and (b), where G_1 is quantized, the dot conductance decreases smoothly as a function of the center gate voltage. In curve (c), G_1 is tuned just below

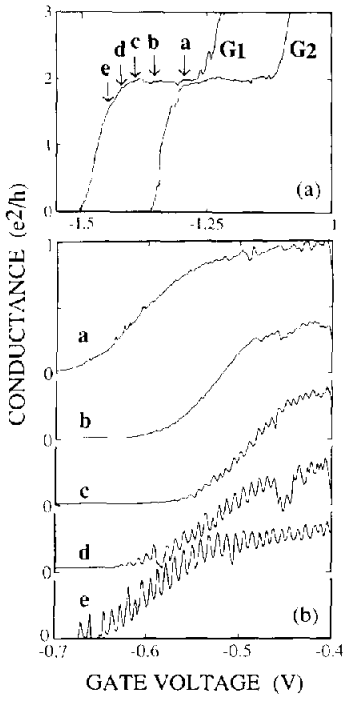

Fig. 3. Comparison of the QPC conductances and the appearance of Coulomb oscillations at zero field. (a) Conductances G_1 and G_2 of the individual QPCs versus gate voltage, both showing a quantized plateau at $2e^2/h$. (b) Conductance of the dot versus center gate voltage V_C for different voltages on QPC_1. The labels 'a' to 'e' correspond with the same labels in the conductance of QPC_1 shown in (a). The conductance G_2 of QPC_2 is fixed below the plateau at about e^2/h. The curves have been offset for clarity.

the plateau and now the dot conductance shows small Coulomb oscillations. The amplitude of the oscillations increases in curve (d) and (e), where the conductance G_1 is reduced further.

A comparison between the individual QPC conductances in fig. 3(a) and the conductance of the dot in fig. 3(b), shows that charging effects at zero field occur only when both QPC conductances are below the quantized plateau value of $2e^2/h$.

At high magnetic fields, when the spin degeneracy is resolved, the conductance of a QPC is quantized in units of e^2/h. Consequently, Coulomb oscillations are expected to appear when both QPCs have a conductance smaller than e^2/h. The dashed curve in fig. 4 shows the

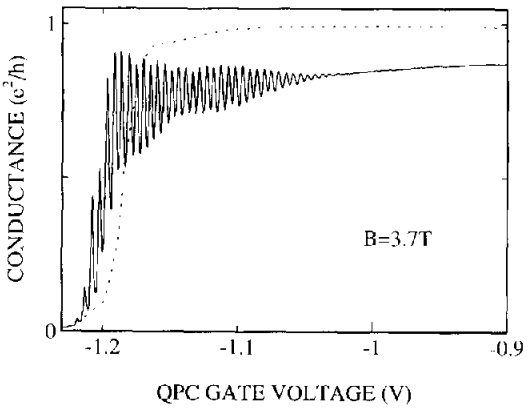

Fig. 4. Dot conductance as a function of the voltage on QPC_1 at a field of 3.9 T with the conductance of QPC_2 kept fixed at $0.9e^2/h$. The dashed curve is the conductance G_1 of QPC_1.

conductance G_1 of QPC_1 at 3.7 T as a function of the gate voltage V_1 on QPC 1. The voltages on the finger gate F and the center gate C_1 are kept constant. G_1 shows a quantized plateau at e^2/h.

The solid curve in fig. 4 shows the dot conductance as a function of the gate voltage V_1 on QPC_1, with QPC_2 set to a conductance of $0.9e^2/h$, i.e. just below the first plateau. For $-1030\,\text{mV} < V_1 < -900\,\text{mV}$, QPC_1 has a quantized conductance of e^2/h and the dot conductance is about constant with a value determined by QPC_2. At $V_1 = -1030$ mV, the conductance of QPC_1 is at the end of the plateau and the dot conductance begins to oscillate. Further decreasing the gate voltage on QPC_1 leads to an increased amplitude of the oscillations. Note that a few maxima exceed the fixed conductance of QPC_2, which is $0.9e^2/h$. This is a signature of resonant tunneling through 0D states.

The experiment of fig. 4 is performed in the regime $G_1, G_2 \lesssim e^2/h$. Earlier experiments in the regime $G_1, G_2 \gtrsim e^2/h$ showed oscillations associated with coherent resonant tunneling through 0D states of the topmost confined Landau level (LL) [2,13]. Alphenaar et al. [14] have pointed out that charging effects can also play a role if $G_1, G_2 \gtrsim e^2/h$, i.e. in the presence of adiabatically transmitted edge channels. In the IQHE regime, charge can be localized in the confined LLs in the dot. The completely transmitted LLs

do not fully screen the charge in the confined LLs. This does not alter the conclusion of ref. [2] that coherent resonant tunneling through 0D states does take place but, beside the 0D energy, one has to include the charging energy to describe the experiment of ref. [2].

At magnetic fields above 8 T, we reach the fractional quantum Hall effect (FQHE) regime in our samples. At these fields, the QPC conductance can be quantized at rational fractions of e^2/h, e.g. $\frac{1}{3}e^2/h$. In fig. 5(a), we have measured the QPC conductance of a different and larger device. The sample, shown in the inset, consists of two QPC gate pairs 1 and 2, and two center gates C. The conductances of QPC_1 and QPC_2 at 11.8 T show a quantized plateau at $\frac{1}{3}e^2/h$. In fig. 5(b) the dot conductance is measured as a function of the voltage on the two center gates C while the QPC voltages are at a fixed value. This experiment is similar to the one at zero field shown in fig. 3. The conductance of QPC_2 is for all curves set to about $0.17e^2/h$. The conductances of QPC_1 are denoted by the arrows in fig. 5(a). The oscillations now appear when both QPC conductances are below the quantized value of $\frac{1}{3}e^2/h$.

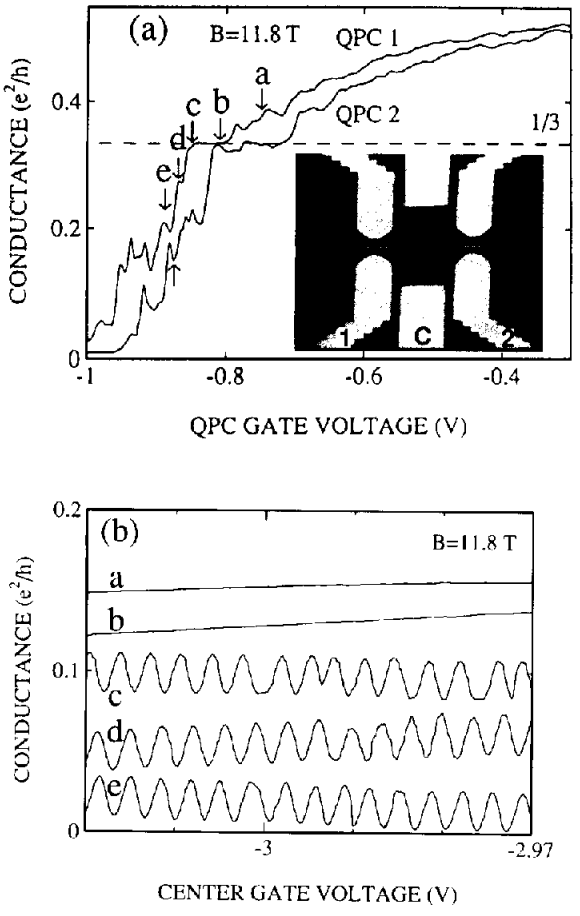

Fig. 5. Comparison of the QPC conductances and the appearance of Coulomb oscillations at a field of 11.8 T. (a) Conductances G_1 and G_2 of the individual QPCs versus gate voltage, both showing a quantized plateau at $\frac{1}{3}e^2/h$. (b) Conductance of the dot versus center gate voltage V_C for different voltages on QPC_1. The labels 'a' to 'e' correspond with the same labels in the conductance of QPC_1 shown in (a). The conductance G_2 of QPC_2 is fixed below the plateau at about $0.15e^2/h$. The curves have been offset for clarity. The inset of (a) shows the gate geometry of the quantum dot with lithographic dimensions of 2.25 μm × 1.5 μm.

The measurements of figs. 3, 4 and 5 show that Coulomb oscillations appear when the conductances of both QPCs are below the first well resolved plateau. Below this plateau, the electrons in the lowest subband have a finite chance to be reflected and the discrete character of the electrons becomes important [10]. This also applies to the FQHE: at the plateau value of $\frac{1}{3}e^2/h$ the transmission probability of the electrons is one. This is in agreement with earlier experiments [15,16] and theory [17]. In those references was shown that transport in the FQHE regime can be described in terms of fractional edge channels.

4.2. *Period and amplitude of the Coulomb oscillations*

The period of the Coulomb oscillations $\Delta V_g = e/C_g$ [18] is determined by the capacitance C_g between the tuned gate and the dot. Applying a magnetic field results in the formation of Landau levels (LLs) in the dot. In a simple one-electron picture edge-states are formed where the LLs intersect the Fermi energy in the dot. In this picture, the Fermi level can lie between LLs, which yields a large incompressible region in the dot. When the Fermi level lines up with a LL, a large compressible region is formed. Therefore,

the capacitance C_g should be larger in the latter case, leading to a smaller Coulomb oscillation period. Below we will show that this simple picture is incorrect by measuring the period of the Coulomb oscillations for different magnetic fields.

First we have examined the period of the Coulomb oscillations over a wide field range, from zero field up to the FQHE regime. Fig. 6 shows the Coulomb oscillations with G_1, $G_2 \ll e^2/h$, as a function of the voltage on the center gate C_1 (see fig. 1). We used different voltages on the QPC gates 1 and 2 for each curve, because the pinch-off voltage of a QPC changes with magnetic field. The voltage on the finger gate F is kept constant at -1 V. The measurements were performed at 35 mK using a dc source–drain voltage of 35 μV. The estimated filling factor of the dot $\nu_{dot} = 1$ for 7.5 T and $\nu_{dot} = 2/3$ for 10 to 11.3 T. We have determined these upper limits for ν_{dot} by measuring the conductance of the dot "area" as a function of the magnetic field, with only a voltage applied to the center gate C_1 and the finger gate F. This measurement shows quantum Hall plateaus, which are shifted to lower fields as compared to the Hall trace of the wide 2DEG due to the reduced electron density in the dot area. The variation in the period of the Coulomb oscillations over the full 0–12 T field range is within 10%. Below we will show that this variation can

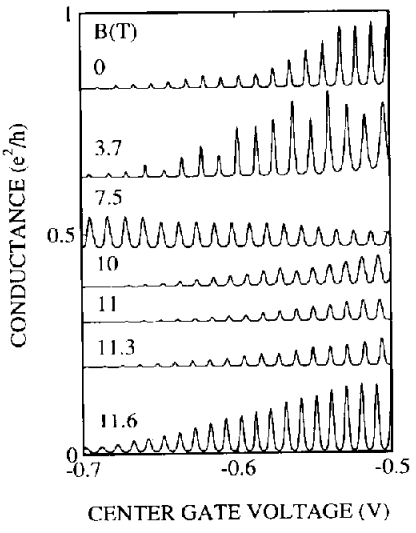

Fig. 6. Dot conductance as a function of the voltage on center gate C_1 for different magnetic fields. The QPC voltages are kept fixed for each individual curve but are not the same for all curves. The curves have been offset for clarity.

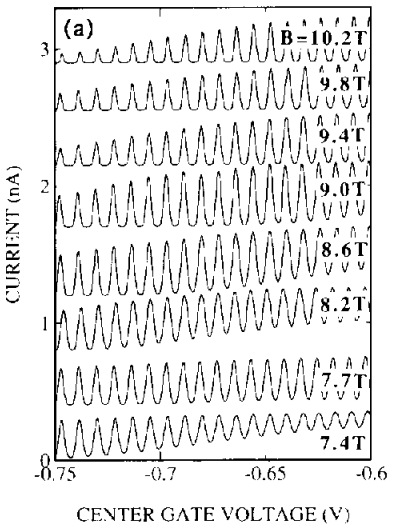

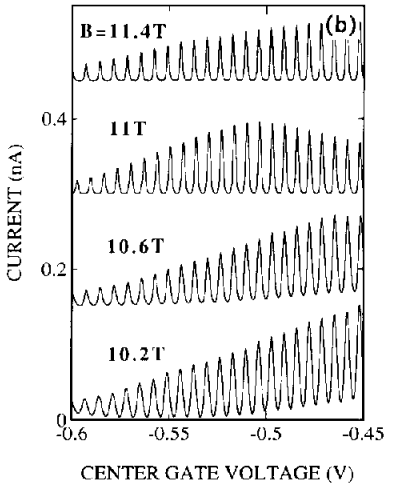

Fig. 7. Current flowing through the dot as a function of the voltage on center gate C_1 for different magnetic fields. In (a), the QPC voltages are kept fixed and are the same for all curves. In (b), the QPC voltages are kept fixed, but at less negative QPC voltages than in (a). The period of the Coulomb oscillations is found to be independent of magnetic field within 1%. The curves have been offset for clarity.

be attributed to the different QPC gate voltages we used for the curves in fig. 6.

In fig. 7(a) the above measurement is repeated over a smaller field range. The voltages on the QPC gates are now the *same* for all curves. The voltage on the finger gate F is kept constant at −0.9 V. At a magnetic field B of 7.4 T and 7.7 T the estimated filling factor $\nu_{dot} = 1$ and for both $B = 9.8$ T, 10.2 T, $\nu_{dot} = 2/3$. The period of the Coulomb oscillations is 7.9 mV, within 1% independent of the filling factor in the dot and is only determined by the capacitance between the center gate and the dot: $C_g = 2.0 \times 10^{-17}$ F.

The dot size increases when the gate voltages are made less negative. Consequently, C_g is expected to increase. In fig. 7(b), the measurement of fig. 7(a) is repeated for higher fields but with less negative QPC gate voltages as in fig. 7. The filling factor $\nu_{dot} = 2/3$ for all fields. Also in this field range, the period of the Coulomb oscillations is field independent. The period is now 6.8 mV which corresponds to a capacitance $C_g = 2.4 \times 10^{-17}$ F. The curves for $B = 10.2$ T in figs. 7(a) and (b) differ only in gate voltage. This shows that the increase of the capacitance C_g is related to the QPC voltages and not to the magnetic field.

The measurements of figs. 6 and 7 show that the period of the Coulomb oscillations is field independent. The formation of LLs in the IQHE regime and a correlated state in the FQHE regime does not influence the gate-to-dot capacitance. This demonstrates that the dot mainly consists of compressible parts. This observation supports a recent self consistent approach to the IQHE [6], where it was shown that only the compressible regions (partially filled LLs) screen the electrostatic potential. This results in large compressible regions separated by small incompressible regions (full LLs).

We now focus on the amplitude of the Coulomb oscillations. The amplitude of the Coulomb oscillations in the curve for $B = 3.7$ T in fig. 6 shows a non-monotonic behaviour. We have measured this effect in more detail at a field of 2.8 T as shown in fig. 8 [12]. In this figure, the temperature and the dc source–drain voltage are reduced to 10 mK and 5 μV, respectively. The

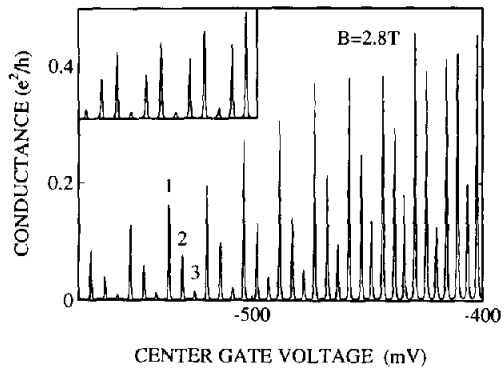

Fig. 8. Dot conductance as a function of the voltage on center gate C_1 at a magnetic field of 2.8 T. In one set of 3 oscillations the peaks are numbered from high to low with 1, 2 and 3. In the inset, the measurement is repeated after bringing the gate voltages to zero. Now, the amplitude of the peaks goes from high to low as the gate voltage is lowered.

conductance of the dot is measured as a function of the center gate voltage, with the other gate voltages kept constant [12]. The conductance shows sharp Coulomb oscillations whose amplitudes are modulated in a very regular way. Note that the same pattern is repeated every three peaks. In one set of three Coulomb oscillations, the peaks are numbered from high to low by 1, 2 and 3. Similar data have been obtained by Staring et al. [19]. They have carried out a detailed analysis of the peak height modulation in high field, which we will use to explain fig. 8.

The Hall conductance of the wide 2DEG is $3e^2/h$ at 3.7 T. There are 3 spin–split LLs in both the ungated 2DEG and the dot. The spatial separation between a LL in the leads and a LL in the dot increases with increasing LL number. This means that the coupling from the leads to a LL in the dot decreases with increasing LL number. Below we will argue that the observed amplitude modulation can be explained if peak 1, 2 and 3 in fig. 8 correspond to tunneling through a particular 0D state belonging to LL1, LL2 and LL3, respectively. This requires a very regular energy spectrum of the quantum dot: in between two 0D states of LL1, a single 0D state of LL2 and LL3 has to be present.

When the Fermi level in the leads lines up with a 0D state from e.g. LL1, the dot conductance shows a Coulomb peak, with an amplitude

determined by the coupling between this state and the leads. By tuning the center gate voltage, the electrostatic energy of the dot is changed and the removal of the next electron is possible. Due to the regular energy spectrum, the Fermi level in the leads will now line up with a discrete state belonging to a higher LL. An elastic tunnel event to this discrete state is energetically possible, but the coupling between this state and the leads is small. Alternatively, transport can take place by thermally assisted tunneling through excited energy states belonging to LL1, which has the largest coupling to the leads. In both cases the amplitude of the oscillation will be smaller than when the Fermi level of the leads lines up with a 0D state in LL1.

After bringing back the gate voltages to zero, we have repeated the measurement of fig. 8. This affects the modulation as shown in the inset of fig. 8. The sequence is now that the amplitude of the peaks goes from high to low as the gate voltage is lowered. This sequence can be obtained from fig. 8 by interchanging e.g. peaks 2 and 3. This indicates that the order of the energy states has changed, but the spectrum is still regular. Switching energy states would not have an effect on the modulation, when thermally assisted tunneling through the 0D states of LL1 is the dominant process for transport. This implies that direct tunneling via a single 0D state is the main contribution to the transport through the dot.

This is also supported by the observation that the transport clearly shows resonant features. The maximum conductance of the Coulomb oscillations in fig. 8 is as high as $0.5e^2/h$, while G_1 and $G_2 < 0.05e^2/h$, indicating that transport takes place through one particular 0D state. Note that the amplitude modulation should disappear when the thermal energy $k_B T$ becomes smaller than the line width of the 0D state. In this case, all peaks will have an amplitude of e^2/h as long as the transmission probability through the left and right barrier are the same.

It is surprising that the peak modulation is not stronger. The coupling from the leads to a LL in the dot decreases by an order of magnitude with increasing LL number. The peak modulation shows only a change in amplitude of about a factor of two. It would be of interest to see if a self consistent approach can account for this discrepancy.

5. Nonlinear measurements: interplay between charging effects and 0D states

In the rather large quantum dots considered so far, the separation between the 0D states of the dot is small on the scale of the charging energy. This separation, as well as the charging energy, increases when the dimensions of the dot are reduced. In this section we study the 0D states in a smaller quantum dot using a source–drain voltage larger than the separation between the 0D states.

The inset of fig. 9 shows a quantum dot with lithographic dimensions of 200 nm × 600 nm. Applying a negative voltage to the gates creates a dot with a diameter d of roughly 100 nm, containing about 25 electrons. We estimate the charging energy $e^2/(4\varepsilon_0\varepsilon_r d)$ to be about 3.5 meV and the single particle level separation to be $E_F/N = 300\ \mu$V, which is an order of magnitude higher in this sample than in the sample shown in fig. 1.

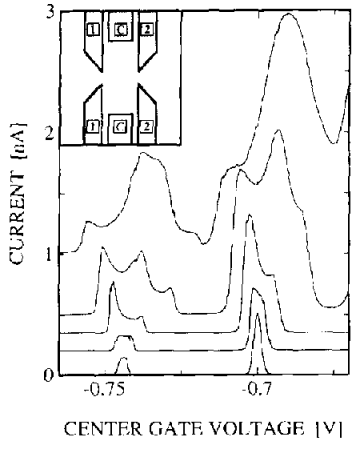

Fig. 9. Current flowing through the dot at a field of 4 T as a function of the voltage on gate C for different source–drain voltages V. From bottom to top, $V = 100$, 200, 400, 700 μV and 1.2 mV. The inset shows the dot geometry with a lithographic size of 200 nm × 600 nm.

Fig. 9 shows the current through the dot as a function of the voltage applied to the center gates C, in a magnetic field of 4 T and for different dc source–drain voltages [20]. From bottom to top, the dc source–drain voltage is increased. The bottom curve is taken in the linear transport regime and shows two normal Coulomb oscillations. In the second curve, these Coulomb oscillations are broadened. In the third curve the oscillations become structured: both oscillations show two maxima and in the fourth curve the oscillations show three maxima. The structure begins to wash out in the top curve.

To explain these results, we have schematically drawn the energy diagram of a quantum dot in fig. 10 for five different gate voltages. The thick vertical lines represent the tunnel barriers induced by the QPCs. The reservoirs are characterized by μ_l and μ_r. The source–drain voltage $V = (\mu_l - \mu_r)/e$ is taken to be somewhat larger than the 0D states separation $\Delta E = E_N - E_{N-1}$.

In fig. 10(a) the number of electrons in the dot is N. Transport through the dot is blocked. Adding one electron to the dot is energetically unfavourable as the addition would increase the conduction band of the dot by e^2/C and lead to a final state of the $(N+1)$th electron which is higher than μ_l and μ_r.

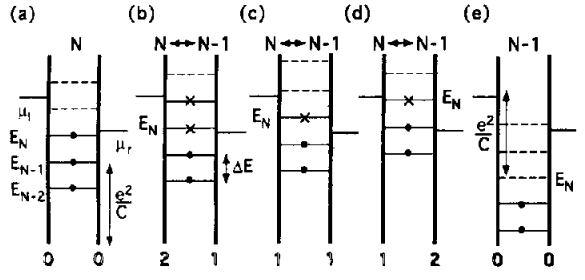

Fig. 10. Energy diagrams of the quantum dot for different gate voltages. The thick vertical lines represent the barriers induced by the QPCs. The number under a barrier is the number of available discrete levels E_N to tunnel to or the number of levels to tunnel out of the dot. The reservoirs are characterized by their electrochemical potentials μ_l and μ_r. The horizontal lines with a black dot denote the occupied 0D states E_N and the dashed horizontal lines denote the empty states. In (a) there are N electrons in the dot and transport is blocked. There are zero levels to tunnel to and zero levels to tunnel out of the dot (0/0). In (b) there are 2 states to tunnel to and there is 1 state to tunnel out of the dot (2/1). The crosses in level E_N and E_{N-1} denote that only one of those levels is occupied. In (c) there is 1 state to tunnel to and 1 state to tunnel from (1/1). In (d) is 1 state to tunnel to and 2 states to tunnel out of the dot (1/2). In (e) are 0 states contributing (0/0). Transport is blocked again and the number of electrons in the dot is now $N-1$.

When the potential of the dot is increased by decreasing the center gate voltage, the 0D states move up with respect to the reservoirs (see fig. 10(b)). The Nth electron can now tunnel to the right reservoir. The non-zero source–drain voltage gives an electron from the left reservoir two choices for tunneling into the dot: it can either tunnel into level E_N *or* E_{N+1}. This is schematically denoted by the crosses in the single particle levels E_N and E_{N+1}. The levels are drawn for the case in which one of those two levels is occupied. Note that when the electron tunnels from the left reservoir to the level E_{N+1}, it can either tunnel out to the right reservoir or first relax into the state E_N.

If the potential of the dot is increased further, the electrons from the left reservoir can only tunnel to level E_N (see fig. 10(c)). Now one level is contributing to the current. Continuing to move up the potential of the dot results in the situation of fig. 10(d). It is still possible to tunnel to level E_N but in this case the electrons in both level E_N and E_{N-1} have a chance to tunnel out of the dot. Moving up the potential further brings the dot back in the situation of the Coulomb blockade (fig. 10(e)).

By going through the different situations from (a) to (c) in fig. 10, we see that the number of states available for transport, changes as 0–2–1–2–0. This is exactly what we observe in the experiment of fig. 9. The third curve shows two maxima corresponding to cases (b) and (d), and a minimum corresponding to case (c). In the same way it is possible to write down a scheme, where the source–drain voltage is somewhat larger than $2\Delta E$. In this case, there will be 2 or 3 states contributing to the current as the center gate voltage is changed and the structured Coulomb oscillation will show 3 maxima and two local minima. This corresponds to the fourth curve in fig. 9 with a source–drain voltage of 700 μV. From this curve we conclude that the

typical level separation ΔE has a value $230\ \mu\text{V} < \Delta E < 350\ \mu\text{V}$, in agreement with the above estimated value from the geometry and electron density of the ungated 2DEG. Similar data have recently been reported by Foxman et al. [21] and Weis et al. [22].

At non-zero source–drain voltage, an asymmetry in the two barrier conductances may be revealed in the total conductance. We will show that, when the tunnel rates through the left barrier Γ_l differs from the tunnel rate through the right barrier Γ_r, the maxima in a structured Coulomb oscillation have different heights. In fig. 11(a), the conductance as a function of the center gate voltage is schematically drawn for the case that $\Gamma_l < \Gamma_r$ and $\mu_l > \mu_r$. The notation x/y in this figure denotes that there are x levels available for the incoming electron and that there are y levels from where an electron can tunnel out of the dot. In the case of fig. 11(a), tunneling into the dot is the bottle neck for transport. For the 1/2 maximum, there is only one state available for the incoming electron, while for the 2/1 maximum, there are two states available. Hence, the 2/1 maximum will be higher than the 1/2 maximum.

To be more quantitative, the 2/1 maximum is proportional to $2\Gamma_l\Gamma_r(2\Gamma_l + \Gamma_r)$ and the 1/2 maximum is proportional to $2\Gamma_l\Gamma_r/(\Gamma_l + 2\Gamma_r)$. We assume here that the tunnel rates are energy independent and that transport takes place by sequential tunneling. For $\Gamma_l < \Gamma_r$, the 2/1 maximum is higher than the 1/2 maximum and vice versa for $\Gamma_l > \Gamma_r$, the 1/2 maximum is higher than the 2/1 maximum (fig. 11(b)).

Transport for the case $2\Delta E \geq eV \geq 3\Delta E$ occurs via the situations 3/1, 2/1, 2/2, 1/2 and 1/3. If $\Gamma_l < \Gamma_r$, we expect the 3/1 maximum to be higher than the 1/3 maximum and vice versa. In order to verify the above arguments, we have measured the structured Coulomb oscillations and adjusted the tunnel rates by changing the voltages on the QPC gates. This is shown in fig. 12 at zero magnetic field. The current through the dot is measured as a function of the center gate C with a dc source–drain voltage V of 1 mV. In the

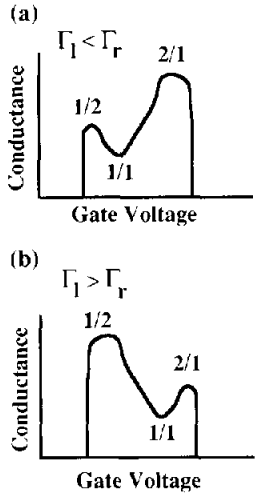

Fig. 11. Schematic plot of the dot conductance as a function of center gate voltage for $\mu_l < \mu_r$. The notation x/y means that there are x levels available for the incoming electron and that there are y levels from where an electron can tunnel out of the dot. In (a) the tunnel rate Γ_l through the left barrier is lower than the tunnel rate Γ_r through the right barrier: $\Gamma_l < \Gamma_r$. In (b), $\Gamma_l < \Gamma_r$; the structure is now reversed.

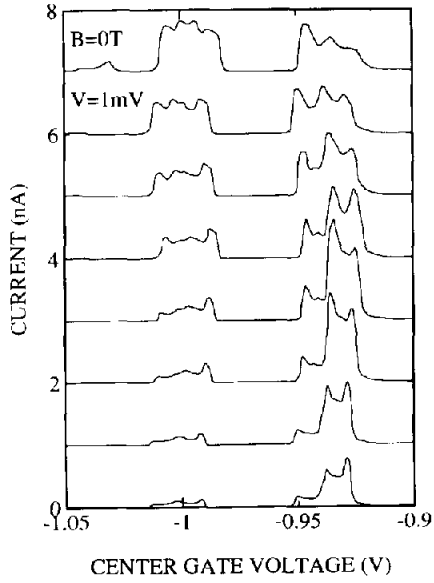

Fig. 12. Current flowing through the dot as a function of the center gate voltage at zero field and a source–drain voltage $V = 1$ mV. In the top curve the conductance of the QPC_1 is higher than the conductance of QPC_2: $\Gamma_l > \Gamma_r$. From top to bottom the conductance of QPC_1 is reduced and the conductance of QPC_2 is increased by changing the QPC voltages. The curves have been offset for clarity.

top curve the conductance of the left barrier is higher than the right barrier ($\Gamma_l > \Gamma_r$). From top to bottom, the gate voltage on the left QPC gate is decreased and the voltage on the right QPC gate is increased in such a way that the potential in the dot is not affected. In the first structured oscillation of the top curve at $V_C \approx -0.93$ V, the 1/3 maximum is higher than the 3/1 maximum ($\Gamma_l > \Gamma_r$). Gradually, the 3/1 peak, which is proportional to $3\Gamma_l\Gamma_r/(3\Gamma_r + \Gamma_2)$, grows and the 1/3 peak, which is proportional to $3\Gamma_l\Gamma_r/(\Gamma_l + 3\Gamma_r)$, decreases as we go from top to bottom. When the 3/1 peak is equal to the 1/3 peak, the tunnel rates through the two barriers are approximately equal: $\Gamma_l \approx \Gamma_r$. The 2/2 peak, which is proportional to $4\Gamma_l\Gamma_r/(2\Gamma_l + 2\Gamma_r)$, is now the highest one. In the bottom curve, the 1/3 maximum is lower than the 3/1 maximum: $\Gamma_l < \Gamma_r$.

The effects are less clear but still present in the second structured oscillation which even shows 4 maxima. If $eV \approx 3\Delta E$, a slight increase in the confinement can result in $3\Delta E \geq eV \geq 4\Delta E$, which would account for the 4 observed maxima. We conclude this section by noting that all the data can be explained qualitatively by our simple model which counts the number of 0D states that can contribute to transport.

6. Discussion and conclusions

Employing the inherent flexibility of gated structures, the conditions to observe charging effects can be studied easily. In this paper, we have shown that Coulomb oscillations appear when the conductance G of both QPCs are below the first plateau: at zero field $G < 2e^2/h$, in the IQHE regime $G < e^2/h$ and in the FQHE regime $G < \frac{1}{3}e^2/h$. For the occurrence of charging effects, the number of electrons in the dot must be a well defined variable. This starts to occur below the first plateau, where the transmission probability of the electrons in the first subband is smaller than one.

Alphenaar et al. [14] have pointed out that in the IQHE regime charging effects can still play a role if the QPC conductances are larger than e^2/h. In this case, charge can be localized in the confined Landau levels in the dot which are separated from each other by magnetically induced tunnel barriers of incompressible electron gas regions. The adiabatically-transmitted-edge channels in the dot do not screen the charge in the confined LLs completely. In this way the Coulomb blockade can also regulate the transport through the dot when $G > e^2/h$, but the temperature dependence and the period of oscillations is different when $G < e^2/h$ [14].

In our quantum dot structures, transport through the dot is mainly determined by the charging energy, but the presence of 0D states strongly influences the shape and the amplitude of the Coulomb oscillations. In the IQHE regime we have found regular amplitude variations which are associated with resonant tunneling through 0D states belonging to different Landau levels. Tunneling to higher LLs suppresses the current and accounts for the regular amplitude variations. As pointed out by Staring et al. [19], this shows that the energy spectrum of a quantum dot can be surprisingly regular.

An interesting point to note is that regular variations in the amplitude of the Coulomb oscillations are also expected in the FQHE regime. This is expected to occur when the confining potentials of the dot are smooth on the scale of the magnetic length. The fractional states at the edges of the dot are then well separated, which leads to the formation of fractional edge channels [15,17]. On the other hand, when the confining potentials are steep, amplitude variations as predicted by Kinaret et al. [7], are expected.

We have used a small quantum dot, containing only 25 electrons, to show that the discrete energy spectrum of the dot results in structured Coulomb oscillations at non-zero source–drain voltages. This voltage lifts the Coulomb blockade for a finite gate voltage interval. The structure in the Coulomb oscillation depends on the 0D states enclosed in the energy window set by the finite source–drain voltage. This reveals the excitation spectrum of the quantum dot for a constant number of electrons in the dot. By tuning the tunnel rates of the QPCs, the struc-

ture of the Coulomb oscillations can be changed showing the effect of asymmetric transmissions of the individual barriers on the conductance of the dot. We explained these measurements with a simple model which counts the number of 0D states contributing to the current.

Acknowledgements

We wish to thank B.M. Alphenaar, C.W.J. Beenakker, L.J. Geerligs, P.L. McEuen, J.E. Mooij, L. Mur, B.J. van Wees and N.S. Wingreen for stimulating discussions, W. Kool for contributions to the device fabrication, and the Delft Institute for MicroElectronics and Submicrotechnology for the use of their facilities. Financial support from FOM and ESPRIT (project 3133, NANSDEV) is gratefully acknowledged.

References

[1] For a review, see: C.W.J. Beenakker and H. van Houten, in: Single Charge Tunneling, eds. H. Grabert, J.M. Martinis and M.H. Devoret (Plenum, New York, 1991).

[2] B.J. van Wees, L.P. Kouwenhoven, C.J.P.M. Harmans, J.G. Williamson, C.E. Timmering, M.E.I. Broekaart, C.T. Foxon and J.J. Harris, Phys. Rev. Lett. 62 (1989) 1523.

[3] M.A. Reed, J.N. Randell, R.J. Aggerwal, R.J. Matyi, T.M. Moore and A.E. Wetsel Phys. Rev. Lett 60 (1988) 535.

[4] For a review, see: D.V. Averin and K.K. Likharev, in: Quantum Effects in Small Disordered Systems, eds. B. Altshuler, P. Lee and R. Webb (North-Holland, Amsterdam, 1990).

[5] P.L. McEuen, E.B. Foxman, U. Meirav, M.A. Kastner, Y. Meir, N.S. Wingreen and S.J. Wind, Phys. Rev. Lett. 66 (1991) 1926.

[6] P.L. McEuen, E.B. Foxman, J.M. Kinaret, U. Meirav, M.A. Kastner, N.S. Wingreen and S.J. Wind, Phys. Rev. B 45 (1992) 11419;
P.L. McEuen, N.S. Wingreen, E.B. Foxman, J. Kinaret, U. Meirav, M.A. Kastner, Y. Meir and S.J. Wind, Physica B 189 (1993) 70.

[7] J.M. Kinaret, N.S. Wingreen, Y. Meir, P.A. Lee and X.-G. Wen, Phys. Rev. B 46 (1992) 4681;
J.M. Kinaret, Physica B 189 (1993) 142.

[8] D.V. Averin, A.N. Korotkov and K.K. Likharev, Phys. Rev. B 44 (1991) 6199.

[9] C.W.J. Beenakker, H. van Houten and A.A.M. Staring, Phys. Rev. B 44 (1991) 1657;
C.W.J. Beenakker, Phys. Rev. B 44 (1991) 1646.

[10] L.P. Kouwenhoven, N.C. van der Vaart, A.T. Johnson, W. Kool, C.J.P.M. Harmans, J.G. Williamson, A.A.M. Staring and C.T. Foxon, Z. Phys. B 85 (1991) 367.

[11] B.J. van Wees, H. van Houten, C.W.J. Beenakker, J.G. Williamson, L.P. Kouwenhoven, D. van der Marel and C.T. Foxon, Phys. Rev. Lett. 60 (1988) 848;
D.A. Wharam, T.J. Thornton, R. Newbury, M. Pepper, H. Ahmed, J.E.F. Frost, D.G. Hasko, D.C. Peacock, D.A. Ritchie and G.A.C. Jones, J. Phys. C 21 (1988) L209.

[12] The measurements of figs. 2 and 9 are actually performed on a sample with a somewhat different gate geometry, see also ref. [10].

[13] L.P. Kouwenhoven, B.J. van Wees, C.J.P.M. Harmans and J.G. Williamson, Surf. Sci. 229 (1990) 290.

[14] B.W. Alphenaar, A.A.M. Staring, H. van Houten, M.A.A. Mabesoone, O.J.A. Buyk and C.T. Foxon, Phys. Rev. B 46 (1992) 76236;
B.W. Alphenaar, A.A.M. Staring, H. van Houten, I.K. Marmorkos, C.W.J. Beenakker and C.T. Foxon, Physica B 189 (1993) 80.

[15] L.P. Kouwenhoven, B.J. van Wees, N.C. van der Vaart, C.J.P.M. Harmans, C.E. Timmering and C.T. Foxon, Phys. Rev. Lett. 64 (1990) 685.

[16] A.M. Chang and J.E. Cunningham, Phys. Rev. Lett. 69 (1992) 2114.

[17] C.W.J. Beenakker, Phys. Rev. Lett. 64 (1990) 216.

[18] This expression is valid in the limit that the separation between the 0D states is much smaller than e^2/C.

[19] A.A.M. Staring, B.M. Alphenaar, H. van Houten, L.M. Molenkamp, O.J.A. Buyk, M.A.A. Mabesoone and C.T. Foxon, Phys. Rev. B, to be published.

[20] A.T. Johnson, L.P. Kouwenhoven, W. de Jong, N.C. van der Vaart and C.J.P.M. Harmans, C.T. Foxon, Phys. Rev. Lett. 69 (1992) 1592.

[21] E.B. Foxman, P.L. McEuen, U. Meirav, N.S. Wingreen, Y. Meir, P.A. Belk, N.R. Belk and M.A. Kastner, to be published;
See also: P.L. McEuen, N.S. Wingreen, E.B. Foxman, J. Kinaret, U. Meirav, M.A. Kastner, Y. Meir and S.J. Wind, Physica B 189 (1993) 70.

[22] J. Weis, R.J. Haug, K. von Klitzing and K. Ploog, Phys. Rev. B 46 (1992) 12837;
J. Weis, R.J. Haug, K. von Klitzing and K. Ploog, Physica B 189 (1993) 111.